



Bi- and trinuclear copper(I) complexes of 1,2,3-triazole-tethered NHC ligands: synthesis, structure, and catalytic properties

Shaojin Gu^{*1}, Jiehao Du¹, Jingjing Huang¹, Huan Xia^{1,2}, Ling Yang¹, Weilin Xu¹ and Chunxin Lu^{*2}

Full Research Paper

[Open Access](#)

Address:

¹School of Materials Science and Engineering, Wuhan Textile University, Wuhan 430200, People's Republic of China and ²College of Biological, Chemical Sciences and Engineering, Jiaying University, Jiaying 314001, People's Republic of China

Email:

Shaojin Gu^{*} - gushaojin@hotmail.com; Chunxin Lu^{*} - chunxin.lu@mail.zjxu.edu.cn

* Corresponding author

Keywords:

copper; CuAAC reaction; N-heterocyclic carbene; 1,2,3-triazole

Beilstein J. Org. Chem. **2016**, *12*, 863–873.

doi:10.3762/bjoc.12.85

Received: 12 January 2016

Accepted: 10 April 2016

Published: 03 May 2016

Associate Editor: I. Marek

© 2016 Gu et al; licensee Beilstein-Institut.

License and terms: see end of document.

Abstract

A series of copper complexes (**3–6**) stabilized by 1,2,3-triazole-tethered N-heterocyclic carbene ligands have been prepared via simple reaction of imidazolium salts with copper powder in good yields. The structures of bi- and trinuclear copper complexes were fully characterized by NMR, elemental analysis (EA), and X-ray crystallography. In particular, $[\text{Cu}_2(\text{L}_2)_2](\text{PF}_6)_2$ (**3**) and $[\text{Cu}_2(\text{L}_3)_2](\text{PF}_6)_2$ (**4**) were dinuclear copper complexes. Complexes $[\text{Cu}_3(\text{L}_4)_2](\text{PF}_6)_3$ (**5**) and $[\text{Cu}_3(\text{L}_5)_2](\text{PF}_6)_3$ (**6**) consist of a triangular Cu_3 core. These structures vary depending on the imidazolium backbone and N substituents. The copper–NHC complexes tested are highly active for the Cu-catalyzed azide–alkyne cycloaddition (CuAAC) reaction in an air atmosphere at room temperature in a CH_3CN solution. Complex **4** is the most efficient catalyst among these polynuclear complexes in an air atmosphere at room temperature.

Introduction

N-Heterocyclic carbene (NHC) have interesting electronic and structural properties. This resulted in their use as versatile ligands in organometallic chemistry and homogeneous catalysis [1–12]. A number of transition metal complexes of NHCs containing pyridine [13], pyrimidine [14], pyrazole [15,16], naphthyridine [17], pyridazine [18], and phenanthroline [19,20] donating groups have been studied in metal-catalyzed organic

transformations. Recently, the easy synthesis and versatile coordination ability of 1,2,3-triazoles have led to an explosion of interest in coordination chemistry [21] and homogeneous catalysis [22–26]. Although a number of metal complexes containing 1,4-disubstituted-1,2,3-triazole ligands were well studied, reports concerning their preparation and use of 1,4-disubstituted-1,2,3-triazoles bearing NHC ligands are rare [22,23].

Elsevier et al. [23] reported several of palladium(II) complexes containing a heterobidentate N-heterocyclic carbene-triazolyl ligand. These palladium(II) complexes are active precatalysts in the transfer semihydrogenation of alkynes to *Z*-alkenes. Messerle et al. [26] synthesized a series of new cationic Rh(I), Rh(III) and Ir(III) complexes containing hybrid bidentate N-heterocyclic carbene-1,2,3-triazolyl donors. We [27] have synthesized a series of nonsymmetrical pincer palladium and platinum complexes containing 1,2,3-triazole-tethered NHC ligands. The obtained palladium complexes displayed high activity in aqueous Suzuki–Miyaura cross-coupling reactions.

We are interested in the synthesis and use of functionalized NHC ligands [20,28–31]. Herein, the synthesis, structural characterization, and catalytic properties of a few copper-1,2,3-triazole-tethered NHC complexes is reported.

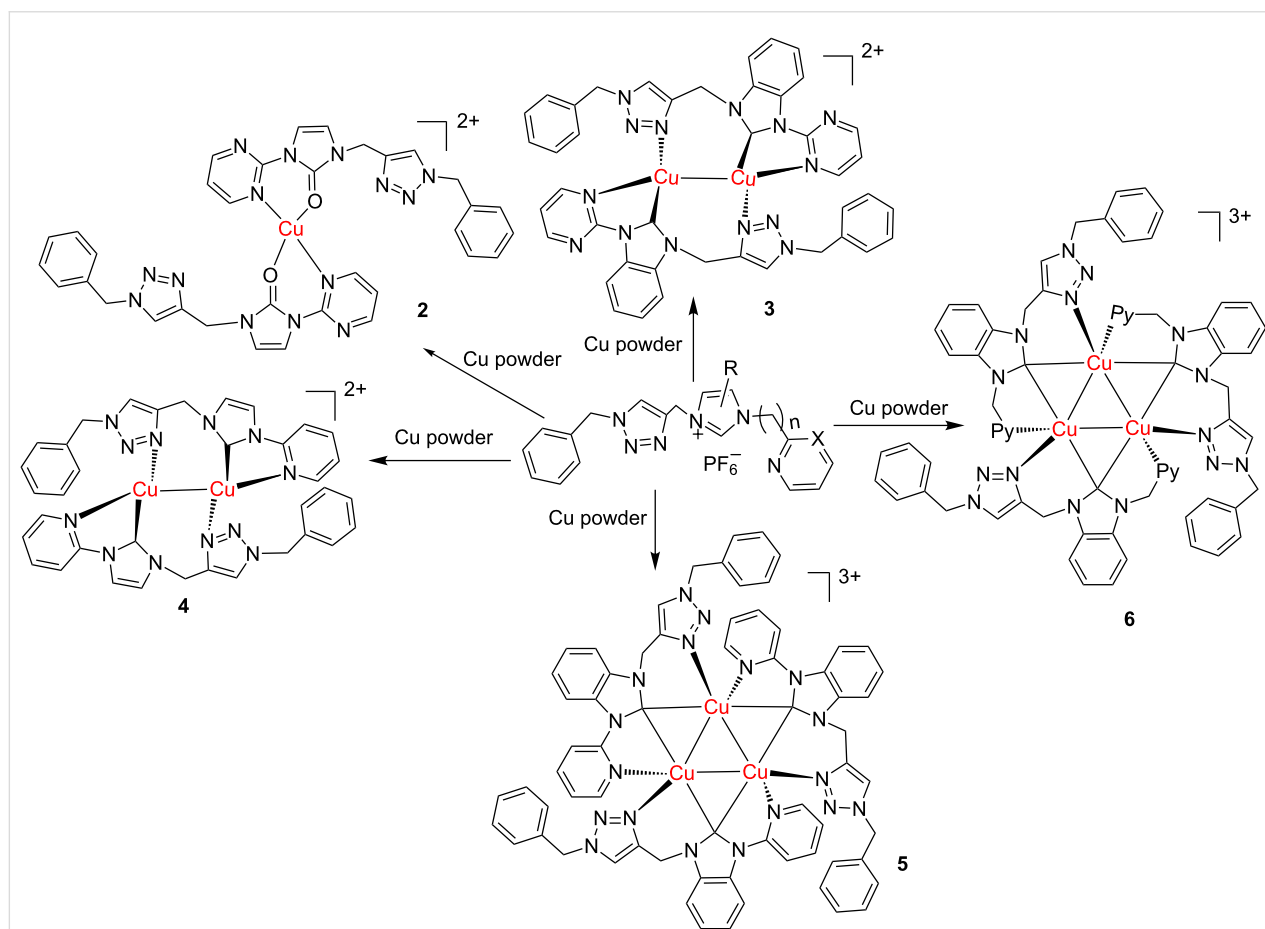
Results and Discussion

Synthesis and spectroscopic characterization

The imidazolium salts (**1a–e**) were prepared according to the reported procedure in 61–90% yields [27]. These imidazolium

salts have been characterized by NMR spectroscopy. The ¹H NMR spectra of these imidazolium salts show singlet peaks between 10.04 and 10.89 ppm in DMSO-*d*₆. As seen in Scheme 1, copper–NHC complexes **3–6** can be obtained in 52–90% yields via directly reacting the corresponding imidazolium salts with an excess of copper powder in CH₃CN at 50 °C for 5 h.

As shown in Scheme 1, reactions of the pyrimidine imidazolium salt **1a** with copper powder in acetonitrile afforded a light yellow Cu(II) complex. In complex **2**, the carbenic carbon atom was oxidized into carbonyl, which is similar with the reported pyrimidyl-imidazole complex [32]. However, a red binuclear Cu(I) complex **3** was obtained in 57% yield when we reacted pyrimidyl benzimidazolium salt **1b** with copper powder. Furtherly, we got a yellow Cu(I)–NHC complex **4** in about 70% yield from pyridine imidazolium salt **1c** and copper powder (Scheme 1). In addition, a triangular Cu(I) complex **6** can be obtained when a flexible ligand was used. Complex **6** consists of a triangular Cu₃ core bridged by three NHCs, which is similar with the published Cu₃ complexes containing flexible



Scheme 1: Synthesis of copper complexes **2–6**.

ligands [33]. Interestingly, we can also obtain a similar triangular Cu_3 complex **5** rather than a binuclear copper complex using a rigid pyridine benzimidazolium salt **1d**. These results demonstrated that the structures vary depending on the N substituents and on the imidazolium backbone. Fine adjustment of the structure of the ligand can lead to different structures.

All of the prepared copper–NHC complexes are stable in air. They were fully characterized by NMR, elemental analysis (EA), and X-ray crystallography. The generation of these copper–NHC complexes were confirmed by the absence of the ^1H NMR resonance signal of the acidic imidazolium protons between 10.04 and 10.89 ppm. The ^1H NMR spectra of all the complexes display only one set of resonance signals assignable to the corresponding ligands, indicating two or three magnetically equivalent ligands. ^{13}C NMR spectra of the copper(I) complexes showed their carbenic carbon resonances at 177.6–191.2 ppm, which are in the normal range of 157.6–216 ppm [34,35].

Single crystal X-ray diffraction studies

To obtain additional insight into the coordination and supramolecular properties, suitable single crystals of all the copper complexes were obtained for single-crystal X-ray diffraction analysis. Crystals were grown by slow diffusion of diethyl ether into an acetonitrile solution of the copper complex at room temperature.

Green-yellow single crystals of complex **2** suitable for an X-ray diffraction study were grown from acetonitrile solution and diethyl ether. The molecular structure of complex **2** in the solid state is depicted in Figure 1 along with the principal bond lengths and angles. Complex **2** crystallizes in the orthorhombic

space group $Pnna$. The remaining atoms of the cation are related by a crystallographic 2-fold symmetry. In complex **2**, the copper ion is four-coordinate in a distorted square planar ligand environment of two nitrogen atoms and two oxygen atoms. The Cu–O bonds are in *trans* configuration and Cu–O distances are shorter than Cu–N distances. The two ligands are arranged in head-to-tail manner. And the $\text{N}_{\text{triazole}}$ did not participate in the coordination.

Single crystals of complex **3** suitable for an X-ray diffraction study were grown from acetonitrile solution and diethyl ether. The molecular structure of complex **3** is depicted in Figure 2.

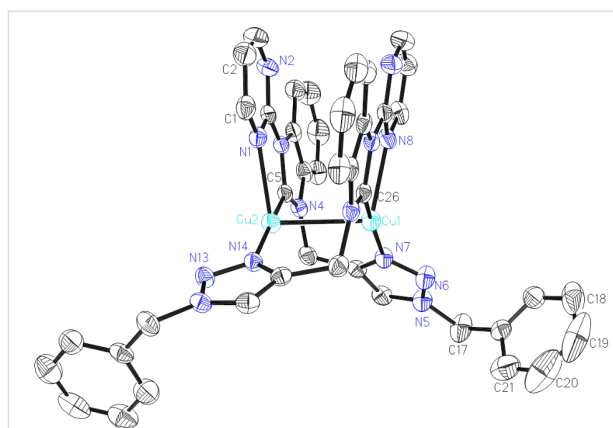


Figure 2: ORTEP the cationic section of $[\text{Cu}_2(\text{L}_2)_2](\text{PF}_6)_2$ (**3**). Thermal ellipsoids are drawn at the 30% probability level. Hydrogen atoms and anions have been removed for clarity. Selected bond distances (Å) and angles ($^\circ$): Cu2–C5 1.896(3), Cu2–N14 1.911(3), Cu2–N1 2.362(3), Cu2–Cu1 2.7867(7), Cu1–C26 1.898(3), Cu1–N7 1.915(3), Cu1–N8 2.340(3), C5–Cu2–N14 173.37(13), C5–Cu2–N1 77.64(13), N14–Cu2–N1 108.15(12), C5–Cu2–Cu1 69.80(9), N14–Cu2–Cu1 111.70(8), N1–Cu2–Cu1 98.90(7), C26–Cu1–N7 167.08(15), C26–Cu1–N8 78.22(13), N7–Cu1–N8 111.77(13), C26–Cu1–Cu2 73.57(9).

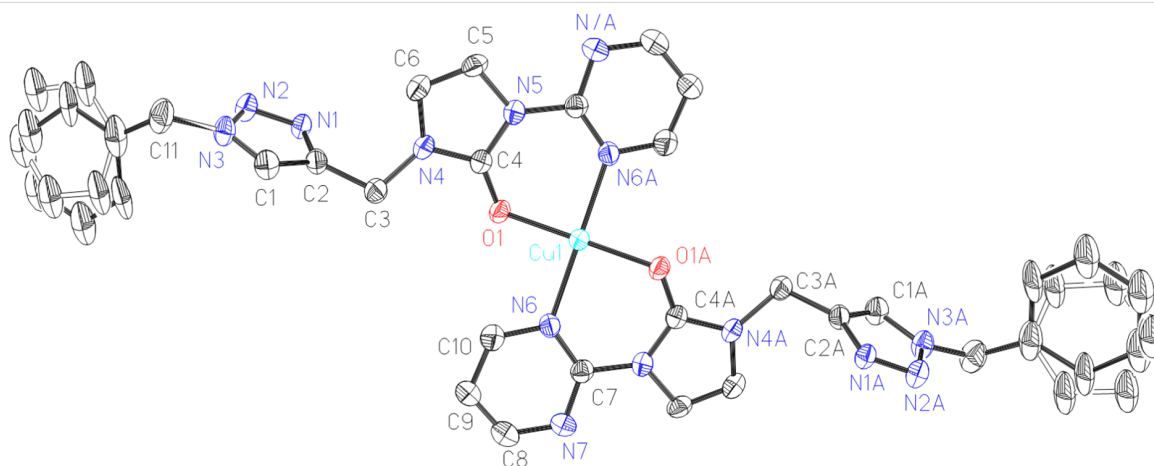


Figure 1: X-ray diffraction structure of copper(II) complex **2** with thermal ellipsoids drawn at 30% probability. The anion and hydrogen atoms are omitted for clarity. Selected bond distances (Å) and angles ($^\circ$): Cu1–O1 1.931(4), Cu1–N6 2.042(5); O1–Cu1–O1A 180.0(3), O1–Cu1–N6A 90.5(2), O1–Cu1–N6 89.5(2), N6–Cu1–N6A 180.00(8). Symmetry transformations used to generate equivalent atoms: $-x, y, 0.5-z$.

Complex **3** crystallizes in the monoclinic space group $C2/c$. The Cu(I) complex contains two crystallographically equivalent Cu centers, which are doubly bridged by two L_2 ligands. The two ligands are arranged in head-to-tail manner. The copper ions are each tri-coordinated by one carbene carbon atom, one nitrogen from pyrimidine, and one nitrogen atom of the triazole rings from two different L_2 ligands. The Cu–carbene bond distances are 1.896(6) and 1.899(5) Å, which are comparable to the known Cu(I)–NHC complexes [36–39]. The Cu1–Cu2 separation is 2.7867(7) Å, showing a weak metal–metal interaction.

The molecular structure of complex **4** is depicted in Figure 3. Complex **4** consists of the cation unit $[Cu_2(L_3)_2]^{2+}$ and two hexafluorophosphate anions. Complex **4** crystallizes in the triclinic space group $P-1$. The two ligands are also arranged in head-to-tail manner. Each copper ion is three-coordinate in a trigonal planar ligand environment of two nitrogen atoms and one NHC carbon center. The Cu–carbene bond distances are 1.888(6) and 1.899(5) Å which are similar with reported copper-carbene complexes (1.85–2.18 Å) [40]. The Cu1–Cu2 separation is 2.6413(12) Å is shorter than in complex **3**, and slightly higher than reported Cu–Cu separations (2.4907 to 2.5150 Å) of the triangular Cu(I)–NHC clusters [33], showing a weak metal–metal interaction.

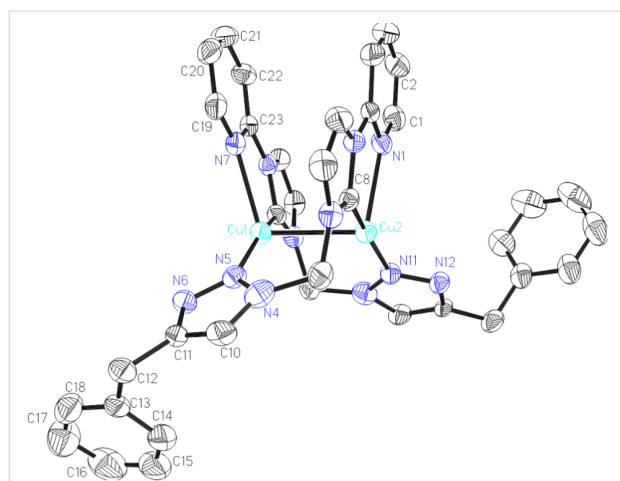


Figure 3: ORTEP drawing of $[Cu_2(L_3)_2](PF_6)_2$ (**4**). Thermal ellipsoids are drawn at the 30% probability level. Hydrogen atoms and anions have been removed for clarity. Selected bond distances (Å) and angles (°): Cu1–C26 1.888(6), Cu1–N5 1.912(5), Cu1–N7 2.289(5), Cu1–Cu2 2.6413(12), Cu2–C8 1.899(5), Cu2–N11 1.922(4), Cu2–N1 2.311(5); C26–Cu1–N5 159.2(2), C26–Cu1–N7 79.0(2), N5–Cu1–N7 116.65(19), C26–Cu1–Cu2 72.49(17), N5–Cu1–Cu2 113.20(15), N7–Cu1–Cu2 105.13(12), C8–Cu2–N11 166.1(2), C8–Cu2–N1 78.6(2), N11–Cu2–N1 110.5(2), C8–Cu2–Cu1 70.45(16), N11–Cu2–Cu1 116.14(15), N1–Cu2–Cu1 102.03(13).

Complex **5** was also characterized via X-ray diffraction. Its structure is shown in Figure 4. Complex **5** consists of two independent molecules in the unit cell. Here, only one molecule was

given in Figure 4. The molecule structure consists of a triangular Cu_3 core bridged by three NHCs ligands. Each NHC forms the 3c-2e bond with two Cu(I) ions with almost equal bond distances (average 2.085 Å), longer than normal Cu–NHC bonds and reported triangular Cu_3 complexes [33,41]. The Cu_3 cores of complex **5** possess nearly equilateral angles close to 60° , whereas in complex **6**, the core is crystallographically restrained to an equilateral triangle. The Cu–Cu distances are around 2.4887 Å and are shorter than that of complex **6**, which may be attributed to more rigid ligand.

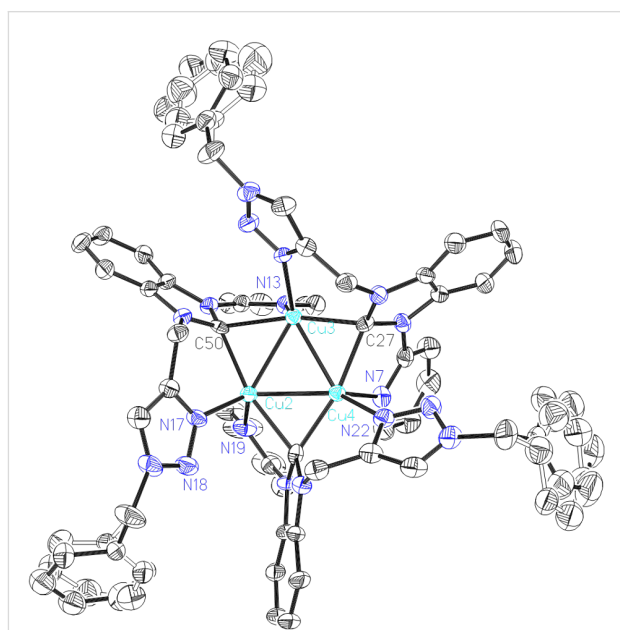


Figure 4: ORTEP drawing of $[Cu_3(L_4)_3](PF_6)_3$ (**5**). Thermal ellipsoids are drawn at the 30% probability level. Hydrogen atoms and anions have been removed for clarity. Selected bond distances (Å) and angles (°): Cu2–N17 2.015(5), Cu2–C50 2.074(6), Cu2–N19 2.107(6), Cu2–C72 2.142(6), Cu2–Cu4 2.4899(11), Cu2–Cu3 2.4928(11), Cu3–N11 2.038(5), Cu3–C27 2.069(6), Cu3–C50 2.113(6), Cu3–N13 2.133(5), Cu3–Cu4 2.4833(10), Cu4–N22 2.043(5), Cu4–C72 2.044(7), Cu4–C27 2.071(6), Cu4–N7 2.086(6); N17–Cu2–C50 94.8(2), N17–Cu2–N19 112.1(2), C50–Cu2–N19 106.8(2), N17–Cu2–C72 93.5(2), C50–Cu2–C72 165.4(2), N19–Cu2–C72 81.0(2), N17–Cu2–Cu4 125.46(18), C50–Cu2–Cu4 113.86(16), N19–Cu2–Cu4 102.90(19), C72–Cu2–Cu4 51.72(17), N17–Cu2–Cu3 129.13(16), C50–Cu2–Cu3 54.18(16), N19–Cu2–Cu3 115.04(17), C72–Cu2–Cu3 111.50(17), Cu4–Cu2–Cu3 59.79(3), N11–Cu3–C27 94.1(2), N11–Cu3–C50 90.9(2), C27–Cu3–C50 163.7(2), N11–Cu3–N13 112.2(2), C27–Cu3–N13 112.1(2), C50–Cu3–N13 80.1(2), N11–Cu3–Cu4 131.09(16), C27–Cu3–Cu4 53.18(17), C50–Cu3–Cu4 112.70(16), N13–Cu3–Cu4 113.70(15), N11–Cu3–Cu2 128.00(15), C27–Cu3–Cu2 112.99(17), C50–Cu3–Cu2 52.76(16), N13–Cu3–Cu2 97.90(16), Cu4–Cu3–Cu2 60.05(3), N22–Cu4–C72 94.4(2), N22–Cu4–C27 92.5(2), C72–Cu4–C27 167.8(2), N22–Cu4–N7 99.9(2), C72–Cu4–N7 107.5(2), C27–Cu4–N7 81.1(2), N22–Cu4–Cu3 134.20(17), C72–Cu4–Cu3 115.49(17), C27–Cu4–Cu3 53.10(17), N7–Cu4–Cu3 102.67(18), N22–Cu4–Cu2 134.48(17), C72–Cu4–Cu2 55.33(17), C27–Cu4–Cu2 113.02(17), N7–Cu4–Cu2 120.11(16), Cu3–Cu4–Cu2 60.16(3).

Complex **6** has also been characterized by single crystal X-ray diffraction (Figure 5). Complex **6** crystallizes in the hexagonal

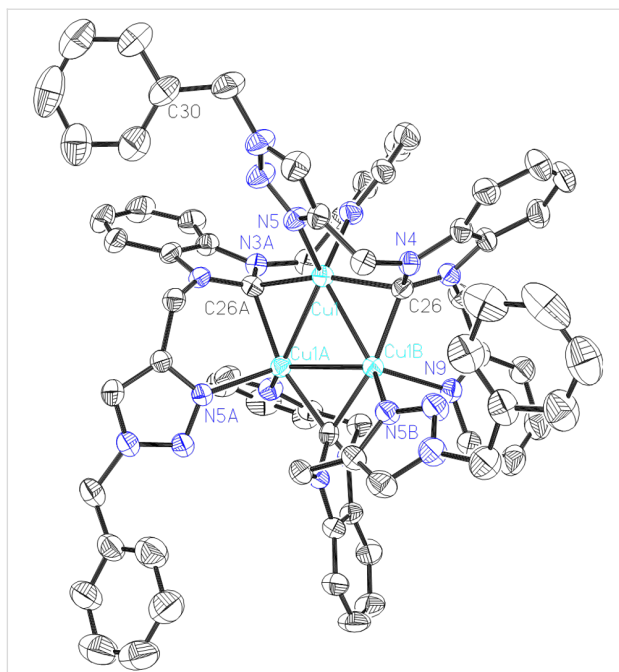


Figure 5: ORTEP drawing of $[\text{Cu}_3(\text{L}_5)_3](\text{PF}_6)_3$ (**6**). Thermal ellipsoids are drawn at the 30% probability level. Hydrogen atoms and anions have been removed for clarity. Selected bond distances (Å) and angles ($^\circ$): Cu1–C26 2.092(6), Cu1–N5 2.092(5), Cu1–C26A 2.024(6), Cu1–N9A 2.152(5), Cu1–Cu1A 2.5141(11), Cu1–Cu1B 2.5141(11); C26–Cu1–N5 101.8(2), C26–Cu1–C26A 163.7(2), N5–Cu1–C26 92.5(2), C26A–Cu1–N9 92.0(2), Cu1–Cu1A–Cu1B 60.0. Symmetry transformations used to generate equivalent atoms: 1–x, 1–y, –z.

space group $R3c$, which is different to the reported trinuclear copper(I) complex containing the symmetric 1,3-bis(2-pyridinylmethyl)benzimidazolyldiene ligand (monoclinic,

$P21/c$) [33] and to the trinuclear copper(I) complex containing a symmetric 1,3-bis(triazole)benzimidazolyldiene ligand (monoclinic, $C2/c$) [38]. Three copper atoms are bridged by three $\text{N}_{\text{pyridine}}\text{CN}_{\text{triazole}}$ NHC ligands forming a Cu_3 ring with three Cu–Cu–Cu angles of 60.0. The geometry of the copper center can be described as distorted trigonal planar. Each copper ion is coordinated by one pyridine, one triazole, and two benzimidazolyldiene ligands displaying a distorted tetrahedral geometry. The Cu–Cu distance is around 2.5145(12) Å showing a weak metal–metal interaction, which is similar with the reported triangle Cu(I) complexes and is shorter than in complexes **3** and **4**. The Cu–N and Cu–C bond distances fall in the range of 2.092(5)–2.152(5) Å and 2.024(6)–2.092(6) Å, respectively, which are slightly longer than in dinuclear complexes **3** and **4**. Benzimidazolyldiene acts as a bridging ligand in a $u2$ mode and bonded equally to two Cu(I) ions, which is only observed in a few silver(I) and copper(I) complexes.

Catalytic application in CuAAC reactions

Inspired by the catalytic activity of Cu(I) species supported by NHC ligand in Cu-catalyzed azide–alkyne cycloaddition (CuAAC) reaction under mild conditions, copper complexes **2–6** were investigated in the CuAAC reaction of azide and phenylacetylene. Firstly, we compared the catalytic activity of different complexes with a complex loading of 0.5 mol %. The reactions were monitored by ^1H NMR analysis at different time points within 4 h (Figure 6). As seen in Figure 6, the yield increased with the extension of reaction time. The results showed that complex **4** displays the best activities for the CuAAC reaction of benzyl azide and phenylacetylene giving a conversion of

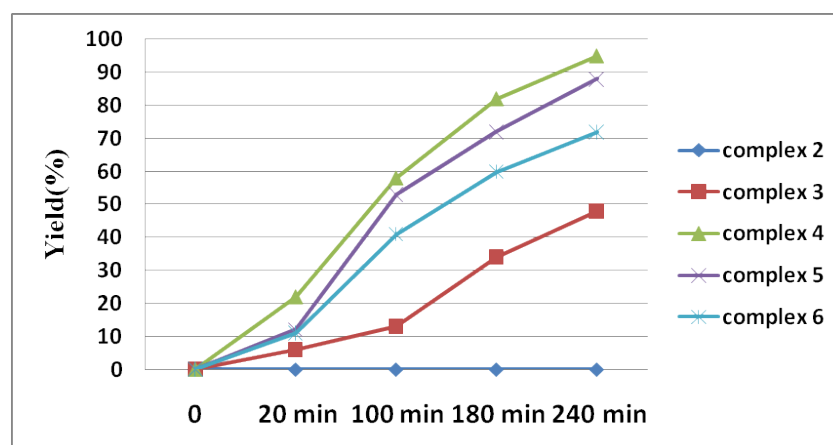
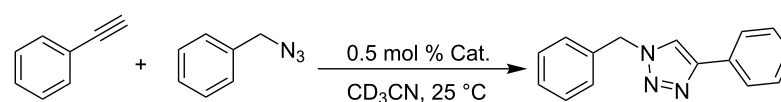


Figure 6: Yield vs reaction time of different copper complex. The reaction was carried out in acetonitrile- d_3 at 25 °C using 0.5 mol % copper complex, yields were determined by ^1H NMR spectra, hexamethylbenzene was used as internal standard.

95%. To further examine the catalytic efficiency of complex **4**, a variation of the catalyst loading from 0.1 to 0.25 to 0.5 mol % within 5 h was performed to give the expected product in yields of 17%, 48%, and 100%. As expected, the coupling reaction with low catalyst loading results in incomplete conversion.

Subsequently the catalytic activity of different solvents was tested at a Cu loading of 0.5 mol % (Table 1). Moderate catalytic activities were obtained for DMSO or without solvent. When CH₃CN was used, the reaction gave an excellent yield (Table 1, entry 4). However, only a moderate yield was obtained when a CH₃CN/H₂O solvent mixture was used (Table 1, entry 6). Thus, CH₃CN was selected as the optimal solvent.

Having optimized the reaction conditions, we extended the CuAAC reaction to other azides and alkynes at room temperature in CH₃CN. As shown in Table 2 (entries 1–5), (azidomethyl)benzene, azidobenzene, (2-azidoethyl)benzene, and 2-(azidomethyl)pyridine could react with phenylacetylene in more than 83% yield (Table 2, entries 1–4). What is more, methyl 1-benzyl-1*H*-1,2,3-triazole-4-carboxylate could be afforded in 85% yield via reacting methyl propiolate with (azidomethyl)benzene. This promising catalytic behavior of complex **4** prompted us to extend our studies toward a one-pot synthesis of 1,2,3-triazoles from alkyl halides, sodium azide, and alkynes. The three-component version has already been successfully performed and described in previous work [20]. As displayed in Table 2, the reactions proceeded smoothly to completion, and the products were isolated in good to excellent yields (83–95%).

Conclusion

In summary, a series of di-, and trinuclear copper(I) complexes (**3–6**) stabilized by 1,2,3-triazole-tethered N-heterocyclic

carbene ligands have been prepared via simple reactions of imidazolium salts with copper powder in good yields. These complexes have been fully characterized by NMR, elemental analysis (EA) and X-ray crystallography. Fine adjustment of the structure of the ligand can lead to different structures. All the Cu–NHC complexes showed high catalyst activity in CuAAC reactions at room temperature. Among these complexes, complex **4** is the most efficient catalyst in an air atmosphere at room temperature.

Experimental

All the chemicals were obtained from commercial suppliers and were used without further purification. Elemental analyses were performed on a Flash EA1112 instrument. ¹H and ¹³C NMR spectra were recorded on a Bruker Avance-400 (400 MHz) spectrometer or a Varian 600 MHz NMR spectrometer. Chemical shifts (δ) are expressed in ppm downfield to TMS at $\delta = 0$ ppm and coupling constants (J) are expressed in Hz.

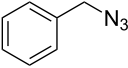
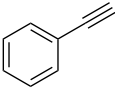
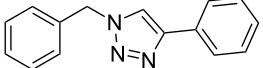
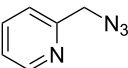
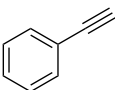
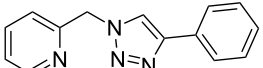
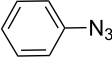
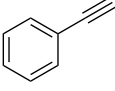
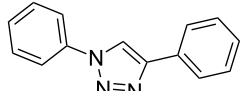
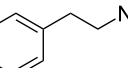
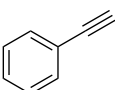
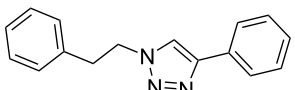
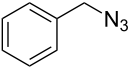
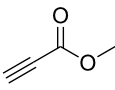
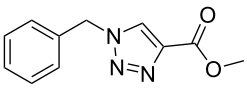
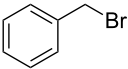
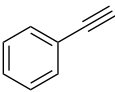
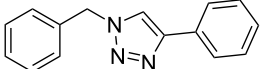
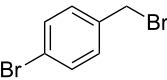
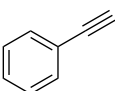
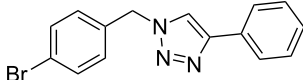
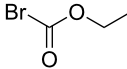
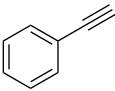
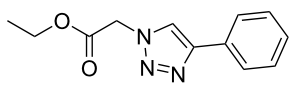
Synthesis of 3-((1-benzyl-1*H*-1,2,3-triazol-4-yl)methyl)-1-(pyrimidin-2-yl)-1*H*-benzo[*d*]imidazol-3-ium hexafluorophosphate [(HL₂)PF₆] (1b**):** Analogously as described in a published work [27], (azidomethyl)benzene (160 mg, 1.2 mmol), copper sulfate pentahydrate (12.5 mg, 0.05 mmol), sodium ascorbate (20 mg, 0.1 mmol), and 3-(prop-2-yn-1-yl)-1-(pyrimidin-2-yl)-1*H*-benzo[*d*]imidazol-3-ium bromide (314 mg, 1 mmol) were added to a Schlenk tube containing 2 mL of water and *tert*-butyl alcohol (1:1). After the heterogeneous mixture was stirred vigorously for 24 h at 50 °C, the reaction mixture was diluted with water (20 mL). The obtained yellow solution was dropwise added to the aqueous solution of NH₄PF₆. A white precipitate was collected by filtration and dried. Yield: 315 mg, 61%. ¹H NMR (400 MHz, DMSO-*d*₆) δ 10.89 (s, 1H), 9.14 (d, $J = 4.9$ Hz, 2H), 8.83 (d, $J = 8.1$ Hz, 1H), 8.39 (s, 1H),

Table 1: CuAAC reaction with different solvents^a.

entry	solvent	cat.	yield % ^b
1	neat	4	50
2	H ₂ O	4	22
3	DMSO	4	53
4	CH ₃ CN	4	95
5	<i>t</i> -BuOH/H ₂ O (1:1)	4	trace
6	CH ₃ CN/H ₂ O (1:1)	4	59

^aReaction carried out using 0.5 mol % of complex **4** with different solvents. ^bYields were determined by ¹H NMR spectra and are reported after 4 h, hexamethylbenzene was used as internal standard.

Table 2: CuAAC Reaction using complex 4 as catalyst.

entry	substrate	substrate	product	isolated yield %
1 ^a				94 [42]
2 ^a				95 [43]
3 ^a				95 [44]
4 ^a				83 [42]
5 ^a				85 [44]
6 ^b				90 [42]
7 ^b				84 [45]
8 ^b				85 [44]

^aReaction conditions: azide 0.5 mmol, ethynylbenzene 0.6 mmol, catalyst 0.5 mol %, CH₃CN 3 mL, rt, 6 h. ^bReaction conditions: alkyl halide 0.5 mmol, NaN₃ 0.6 mmol, ethynylbenzene 0.6 mmol, catalyst 0.5 mol %, CH₃CN/H₂O 1:1 (3 mL), rt, 16 h.

8.17 (d, $J = 8.0$ Hz, 1H), 7.79 (br, 3H), 7.34–7.30 (m, 5H), 6.06 (s, 2H), 5.63 (s, 2H); ¹³C NMR (101 MHz, DMSO-*d*₆) δ 160.34, 159.78, 143.41, 140.45, 136.12, 132.14, 129.62, 129.26, 128.69, 128.49, 127.79, 125.52, 53.47, 42.95.

Synthesis of 3-((1-benzyl-1H-1,2,3-triazol-4-yl)methyl)-1-(pyridin-2-yl)-1H-imidazol-3-ium hexafluorophosphate [(HL₃)PF₆] (1c): Similarly as described in a previous procedure [27], a mixture of (azidomethyl)benzene (160 mg, 1.2 mmol), copper sulfate pentahydrate (12.5 mg, 0.05 mmol) and sodium ascorbate (20 mg, 0.1 mmol), 3-(prop-2-ynyl)-1-(pyridin-2-yl)-1H-imidazol-3-ium bromide (265 mg, 1 mmol) was added to 2 mL of water and *tert*-butyl alcohol (1:1). The heterogeneous mixture was stirred vigorously for 24 h at 50 °C. The reaction mixture was diluted with water (20 mL), and the yellow solution was dropwise added to the aqueous solution of NH₄PF₆. A white precipitate was collected by filtration and dried. Yield: 415 mg, 90%. ¹H NMR (400 MHz, DMSO-*d*₆) δ 10.19 (s, 1H), 8.69–8.63 (m, 1H), 8.54 (t, $J = 1.9$ Hz, 1H), 8.35

(d, $J = 2.4$ Hz, 1H), 8.31–8.17 (m, 1H), 8.03 (q, $J = 4.3, 3.5$ Hz, 2H), 7.70–7.61 (m, 1H), 7.36 (qd, $J = 7.0, 6.5, 2.5$ Hz, 5H), 5.65 (dd, $J = 5.1, 2.4$ Hz, 4H), 3.39 (s, 1H); ¹³C NMR (101 MHz, DMSO-*d*₆) δ 149.69, 146.78, 141.06, 141.02, 135.68, 129.29, 128.76, 128.55, 125.77, 125.23, 124.14, 120.07, 114.75, 53.49, 44.85.

Synthesis of 3-((1-benzyl-1H-1,2,3-triazol-4-yl)methyl)-1-(pyridin-2-yl)-1H-benzo[d]imidazol-3-ium hexafluorophosphate [(HL₄)PF₆] (1d): Similarly as described in a previous procedure [27], the imidazolium salt was prepared similarly as for [(HL₃)PF₆] from (azidomethyl)benzene (160 mg, 1.2 mmol), copper sulfate pentahydrate (12.5 mg, 0.05 mmol), sodium ascorbate (20 mg, 0.1 mmol), and 3-(prop-2-yn-1-yl)-1-(pyridin-2-yl)-1H-benzo[d]imidazol-3-ium bromide (314 mg, 1 mmol). Yield: 317 mg, 62%. ¹H NMR (400 MHz, DMSO-*d*₆) δ 10.60 (s, 1H), 8.75 (d, $J = 4.7$ Hz, 1H), 8.46–8.31 (m, 2H), 8.25 (t, $J = 8.0$ Hz, 1H), 8.19–8.10 (m, 1H), 8.02 (d, $J = 8.2$ Hz, 1H), 7.79–7.65 (m, 3H), 7.31 (dt, $J = 21.5, 7.4$ Hz, 7H), 5.95 (s,

2H), 5.59 (d, $J = 5.1$ Hz, 2H); ^{13}C NMR (101 MHz, DMSO- d_6) δ 149.97, 147.61, 143.07, 141.07, 140.46, 136.13, 131.72, 130.09, 129.27, 128.74, 128.50, 128.30, 127.73, 125.73, 125.50, 117.68, 116.38, 114.80, 53.42, 42.83.

Synthesis of 3-((1-benzyl-1*H*-1,2,3-triazol-4-yl)methyl)-1-(pyridin-2-ylmethyl)-1*H*-benzo[*d*]imidazol-3-ium hexafluorophosphate [(HL₅)PF₆] (1e): Similarly as described in previous procedure [27], the imidazolium salt was prepared similarly as for [(HL₃)PF₆] from (azidomethyl)benzene (160 mg, 1.2 mmol), and 3-(prop-2-yn-1-yl)-1-(pyridin-2-ylmethyl)-1*H*-benzo[*d*]imidazol-3-ium bromide (328 g, 1 mmol). Yield: 390 mg, 74%. ^1H NMR (400 MHz, DMSO- d_6) δ 10.04 (s, 1H, NCHN), 8.46 (d, $J = 4.8$ Hz, 1H, 2-Py), 8.39 (s, 1H, triazole), 8.10 (d, $J = 8.0$ Hz, 1H, 4-Py), 7.94–7.90 (m, 3H), 7.73–7.59 (m, 3H), 7.46–7.27 (m, 6H, phenyl+benzene), 5.95 (s, 4H, CH₂), 5.63 (s, 2H, CH₂); ^{13}C NMR (101 MHz, DMSO- d_6) δ 153.34, 150.04, 143.67, 140.07, 138.02, 136.14, 131.80, 131.29, 129.27, 128.74, 128.48, 127.33, 127.16, 125.33, 124.19, 123.20, 114.48, 114.41, 53.5, 51.4, 42.3.

General procedure for the preparation of Cu(I)–NHC complexes and Cu(II) complex: Analogously as described in [39], all the copper complexes were prepared by the following route: imidazolium salt (0.2 mmol) and an excess of copper powder (64 mg, 1.0 mmol) were placed in 3 mL of MeCN to form a heterogeneous mixture solution. After the mixture was stirred at 50 °C for 10 h under air, the solution was filtered through Celite. Single crystals suitable for X-ray diffraction analysis were grown from acetonitrile solution and diethyl ether.

Synthesis of [Cu-((1-benzyl-1*H*-1,2,3-triazol-4-yl)methyl)-3-(pyrimidin-2-yl)-1,3-dihydro-2*H*-imidazol-2-one)]₂(PF₆)₂ (2): This complex was synthesized by the reaction of [H(L₁)](PF₆) (1a; 93 mg, 0.2 mmol) with copper powder (64 mg, 1.0 mmol) at 50 °C for 10 h. Yield: 79 mg (75%), light green crystals. Anal. calcd for C₃₄H₃₀CuF₁₂N₁₄O₂P₂. 0.5 CH₃CN: C, 40.39; H, 3.05; N, 19.52; found: C, 40.73; H, 2.95; N, 19.15.

Synthesis of [Cu₂(L₂)₂](PF₆)₂ (3): This complex was synthesized by the reaction of [HL₂](PF₆) (1b; 102 mg, 0.2 mmol) with copper powder (64 mg, 1.0 mmol) at 50 °C for 10 h. Yield: 66 mg (57%), red crystals. ^1H NMR (600 MHz, acetonitrile- d_3) δ 8.75 (d, $J = 8.1$ Hz, 2H, benzimidazole), 8.70 (d, $J = 4.9$ Hz, 4H, pyrimidine), 7.88 (s, 2H, triazole), 7.79 (d, $J = 7.8$ Hz, 2H, benzimidazole), 7.59–7.54 (m, 2H, benzimidazole), 7.52 (t, $J = 7.2$ Hz, 2H, benzimidazole), 7.36 (t, $J = 4.9$ Hz, 2H, pyrimidine), 7.31–7.29 (m, 6H, phenyl), 7.19–7.18 (m, 4H, phenyl), 5.61 (s, 4H, -CH₂-), 5.38 (s, 4H, -CH₂-); ^{13}C NMR (151 MHz, acetonitrile- d_3) δ 191.23 (Cu-C), 158.73, 157.33, 142.39, 136.17

135.75, 132.61, 129.94, 129.67, 129.17, 126.34, 126.19, 125.58, 120.66, 116.95, 112.75, 54.12, 43.41; Anal. calcd for C₄₂H₃₄Cu₂F₁₂N₁₄P₂: C, 43.80; H, 2.98; N, 17.02; found: C, 43.51; H, 2.85; N, 16.95.

Synthesis of [Cu₂(L₃)₂](PF₆)₂ (4): The compound was prepared similarly as for complex 3 from [HL₃](PF₆) (90 mg, 0.20 mmol) with copper powder (64 mg, 1.0 mmol) at 50 °C for 10 h, orange yellow solid. Yield: 71 mg, 68%. ^1H NMR (600 MHz, acetonitrile- d_3) δ 7.96 (s, 1H, triazole), 7.90 (br, 1H, 2-py), 7.83 (br, 1H, imidazole), 7.76 (s, 1H, 4-py), 7.57 (br, 1H, imidazole), 7.41 (s, 1H, 5-py), 7.37 (d, $J = 7.8$ Hz, 3H, phenyl), 7.30–7.22 (m, 3H, phenyl + 3-py), 5.47 (s, 2H), 5.38 (s, 2H); ^{13}C NMR (151 MHz, acetonitrile- d_3) δ 181.20 (Cu-C), 149.68, 147.26, 140.72, 138.41, 134.71, 129.02, 128.89, 128.80, 128.28, 128.04, 123.96, 123.48, 112.13, 54.36, 45.69; Anal. calcd for C₃₆H₃₂Cu₂F₁₂N₁₂P₂: C, 41.19; H, 3.07; N, 16.01; found: C, 41.25; H, 3.31; N, 15.46.

Synthesis of [Cu₃(L₄)₃](PF₆)₃ (5): The compound was prepared similarly as for complex 3 from [HL₄](PF₆) (106 mg, 0.20 mmol) with copper powder (64 mg, 1.0 mmol) at 50 °C for 10 h, light yellow solid. Yield: 93 mg, 52%. ^1H NMR (600 MHz, acetone- d_6) δ 8.77 (d, $J = 8.1$ Hz, 1H, 2-py), 8.46 (td, $J = 8.0, 1.8$ Hz, 1H, 4-py), 8.33 (s, 1H, triazole), 8.23–8.20 (m, 1H), 7.90 (dd, $J = 5.1, 1.5$ Hz, 1H, benzimidazole), 7.84–7.81 (m, 1H, benzimidazole), 7.68–7.60 (m, 2H, benzimidazole), 7.44 (dd, $J = 7.6, 5.0$ Hz, 1H, 5-py), 7.33–7.31 (m, 3H, phenyl), 6.94–6.92 (m, 2H, phenyl), 5.84 (d, $J = 15.8$ Hz, 1H), 5.37 (d, $J = 15.8$ Hz, 1H), 5.18 (s, 2H); ^{13}C NMR (151 MHz, DMSO- d_6) δ 178.99 (Cu-C), 149.61, 148.44, 142.25, 140.55, 136.19, 134.91, 133.34, 129.31, 128.93, 128.09, 126.05, 125.82, 124.48, 124.27, 119.09, 118.51 (CH₃CN), 112.74, 111.59, 54.13, 41.17, 1.56(CH₃CN); Anal. calcd for C₁₃₂H₁₀₈Cu₆F₃₆N₃₆P₆. 3CH₃CN: C, 46.39; H, 3.30; N, 15.29; found: C, 45.87; H, 3.40; N, 15.30.

Synthesis of [Cu₃(L₅)₃](PF₆)₃ (6): The compound was prepared similarly as for complex 3 from [HL₅](PF₆) (106 mg, 0.20 mmol) with copper powder (64 mg, 1.0 mmol) at 50 °C for 10 h, light yellow solid. Yield: 106 mg, 90%. ^1H NMR (600 MHz, nitromethane- d_3) δ 8.13 (s, 1H, triazole), 7.92 (td, $J = 7.8, 1.8$ Hz, 1H, pyridine), 7.77 (d, $J = 7.8$ Hz, 1H, pyridine), 7.59 (d, $J = 7.8$ Hz, 1H, pyridine), 7.61–7.36 (m, 6H, phenyl + benzimidazole), 7.14–7.08 (m, 2H, benzimidazole), 6.95 (ddd, $J = 7.5, 5.2, 1.1$ Hz, 1H, pyridine), 6.49–6.45 (d, $J = 4.8$ Hz, 1H, benzimidazole), 5.40 (d, $J = 15.0$ Hz, 1H, -CH₂-), 5.30 (d, $J = 15.0$ Hz, 1H, -CH₂-), 5.27 (d, $J = 15.0$ Hz, 1H, -CH₂-), 5.26 (d, $J = 15.6$ Hz, 1H, -CH₂-), 5.21 (d, $J = 15.0$ Hz, 1H, -CH₂-), 4.98 (d, $J = 15.6$ Hz, 1H, -CH₂-); ^{13}C NMR (150 MHz, nitromethane- d_3) 177.57 (Cu-C), 151.99, 148.85,

141.78, 139.93, 135.15, 134.68, 133.85, 129.16, 128.98, 128.81, 128.12, 125.04, 124.62, 124.35, 123.79, 110.58, 110.26, 54.49, 51.29, 40.72; Anal. calcd for $C_{69}H_{60}Cu_3F_{18}N_{18}P_3$: C, 46.90; H, 3.42; Cu, 10.79; N, 14.27; found: C, 46.35; H, 3.31; N, 13.95.

General procedure for the copper-catalyzed CuAAC reaction: Analogously as described in [31], in a 10 mL Schlenk tube, azide (0.5 mmol), alkyne (0.6 mmol), and 0.5 mol % copper complex were dissolved in 3.0 mL of CH_3CN . After the mixture was stirred at rt under air for a desired time, the reaction was stopped by the addition of H_2O (2 mL) to the resultant mixture. Then the mixture was extracted with CH_2Cl_2 . The organic layer was separated from the aqueous phase. After the organic phase was dried over $MgSO_4$, the solution was filtered and concentrated under vacuum. The residue was purified by flash chromatography (silica gel, petroleum ether/ethyl acetate, 3:1) to give the desired product

X-ray diffraction analysis

Analogously as described in [27], single-crystal X-ray diffraction data were collected at 298(2) K on a Siemens Smart/CCD area-detector or Oxford Diffraction Gemini A Ultra diffractometer with a Mo $K\alpha$ radiation ($\lambda = 0.71073 \text{ \AA}$) by using an ω - 2θ scan mode. Unit-cell dimensions were obtained with least-squares refinement. Data collection and reduction were performed using the SMART and SAINT software [46]. The structures were solved by direct methods, and the non-hydrogen atoms were subjected to anisotropic refinement by full-matrix least squares on F_2 using the SHELXTXL package [47]. Hydro-

gen atom positions for all of the structures were calculated and allowed to ride on their respective C atoms with the C–H distances of 0.93–0.97 \AA and $U_{iso}(H) = 1.2 - 1.5U_{eq}(C)$. Disordered solvent molecules that could not be modeled successfully were removed with SQUEEZE [48]. Further details of the structural analysis are summarized in Table 3.

Supporting Information

Supporting Information File 1

X-ray crystallographic data in cif format CCDC 1424013–1424017.

[<http://www.beilstein-journals.org/bjoc/content/supplementary/1860-5397-12-85-S1.cif>]

Acknowledgements

The authors thank the National Natural Science Foundation of China (21202127), and the Educational Commission of the Hubei Province (Q20151606) for financial support. Shaojin Gu gratefully acknowledges financial support from the China Scholarship Council (201308420278).

References

1. Díez-González, S.; Marion, N.; Nolan, S. P. *Chem. Rev.* **2009**, *109*, 3612–3676. doi:10.1021/Cr900074m
2. Poyatos, M.; Mata, J. A.; Peris, E. *Chem. Rev.* **2009**, *109*, 3677–3707. doi:10.1021/Cr800501s

Table 3: Crystallographic data for complexes 2–6.

	2	3	4	5	6
CCDC number	1424013	1424014	1424015	1424016	1424017
formula	$C_{70}H_{63}Cu_2F_{24}N_{29}O_4P_4$	$C_{42}H_{34}Cu_2F_{12}N_{14}P_2$	$C_{36}H_{32}Cu_2F_{12}N_{12}P_2$	$C_{278}H_{237}Cu_{12}F_{72}N_{79}P_{12}$	$C_{69}H_{60}Cu_3F_{18}N_{18}P_3$
Fw.	2081.47	1161.93	1049.76	7186.59	1766.88
crystal system	orthorhombic	monoclinic	triclinic	hexagonal	hexagonal
space group	<i>Pnna</i>	<i>C2/c</i>	<i>P-1</i>	<i>R3c</i>	<i>R3c</i>
<i>a</i> / \AA	14.0847(15)	34.298(3)	12.9626(10)	28.178(3)	21.4692(13)
<i>b</i> / \AA	14.5426(16)	13.2602(12)	13.0382(9)	28.178(3)	21.4692(13)
<i>c</i> / \AA	22.599(2)	26.605(4)	13.1663(10)	16.3997(19)	71.858(9)
β /deg	90.00	129.8310(10)	80.661(6)	90.00	90.00
$V/\text{\AA}^3$	4629.0(9)	9291.9(19)	2111.7(3)	45655(10)	28684(4)
<i>Z</i>	2	8	2	6	12
<i>D</i> /g cm^{-3}	1.493	1.661	1.651	1.568	1.228
Reflns collected	18121	10632	7571	21009	5624
ind reflns, <i>R</i> _{int}	12510, 0.0545	7828, 0.0250	4679, 0.0467	15722, 0.0869	3716, 0.0650
goodness-of-fit on <i>F</i> ²	1.063	1.018	1.023	1.031	1.157
<i>R</i> ₁ , <i>wR</i> ₂ [<i>I</i> > 2 σ (<i>I</i>)]	0.0869, 0.2496	0.0562, 0.1652	0.0696, 0.1774	0.0622, 0.1353	0.0688, 0.2044
<i>R</i> ₁ , <i>wR</i> ₂ (all data)	0.1338, 0.3001	0.0779, 0.1858	0.1122, 0.2172	0.0917, 0.1543	0.1200, 0.2623

3. Bernhammer, J. C.; Han Vinh, H. *Organometallics* **2014**, *33*, 1266–1275. doi:10.1021/om500083r
4. Farrell, K.; Albrecht, M. Late Transition Metal Complexes with Pincer Ligands that Comprise N-Heterocyclic Carbene Donor Sites. In *The Privileged Pincer-Metal Platform: Coordination Chemistry & Applications*; van Koten, G.; Gossage, R. A., Eds.; Springer: Berlin, Germany, 2016; pp 45–91.
5. Velazquez, H. D.; Verpoort, F. *Chem. Soc. Rev.* **2012**, *41*, 7032–7060. doi:10.1039/c2cs35102a
6. Gaillard, S.; Cazin, C. S. J.; Nolan, S. P. *Acc. Chem. Res.* **2012**, *45*, 778–787. doi:10.1021/ar200188f
7. Lazreg, F.; Nahra, F.; Cazin, C. S. J. *Coord. Chem. Rev.* **2015**, *293*, 48–79. doi:10.1016/j.ccr.2014.12.019
8. Prakasham, A. P.; Ghosh, P. *Inorg. Chim. Acta* **2015**, *431*, 61–100. doi:10.1016/j.ica.2014.11.005
9. Mata, J. A.; Hahn, F. E.; Peris, E. *Chem. Sci.* **2014**, *5*, 1723–1732. doi:10.1039/c3sc53126k
10. Fortman, G. C.; Nolan, S. P. *Chem. Soc. Rev.* **2011**, *40*, 5151–5169. doi:10.1039/c1cs15088j
11. Mejuto, C.; Royo, B.; Guisado-Barrios, G.; Peris, E. *Beilstein J. Org. Chem.* **2015**, *11*, 2584–2590. doi:10.3762/bjoc.11.278
12. Schulte to Brinke, C.; Hahn, F. E. *Dalton Trans.* **2015**, *44*, 14315–14322. doi:10.1039/c5dt02115d
13. Ibrahim, H.; Bala, M. D. *J. Organomet. Chem.* **2015**, *794*, 301–310. doi:10.1016/j.jorganchem.2015.07.015
14. Chen, C.; Lu, C.; Zheng, Q.; Ni, S.; Zhang, M.; Chen, W. *Beilstein J. Org. Chem.* **2015**, *11*, 1786–1795. doi:10.3762/bjoc.11.194
15. Liu, B.; Liu, B.; Zhou, Y.; Chen, W. *Organometallics* **2010**, *29*, 1457–1464. doi:10.1021/om100009u
16. Guo, T.; Dechert, S.; Meyer, F. *Organometallics* **2014**, *33*, 5145–5155. doi:10.1021/om500351j
17. Zhang, X.; Xi, Z.; Liu, A.; Chen, W. *Organometallics* **2008**, *27*, 4401–4406. doi:10.1021/om8003674
18. Liu, X.; Chen, W. *Organometallics* **2012**, *31*, 6614–6622. doi:10.1021/om300644h
19. Gu, S.; Liu, B.; Chen, J.; Wu, H.; Chen, W. *Dalton Trans.* **2012**, *41*, 962–970. doi:10.1039/c1dt11269d
20. Gu, S.; Xu, D.; Chen, W. *Dalton Trans.* **2011**, *40*, 1576–1583. doi:10.1039/c0dt01211d
21. Crowley, J.; McMorran, D. “Click-Triazole” Coordination Chemistry: Exploiting 1,4-Disubstituted-1,2,3-Triazoles as Ligands. In *Click Triazoles*; Košmrlj, J., Ed.; Springer: Berlin, Germany, 2012; pp 31–83.
22. Sluijter, S. N.; Elsevier, C. J. *Organometallics* **2014**, *33*, 6389–6397. doi:10.1021/om5007038
23. Warsink, S.; Drost, R. M.; Lutz, M.; Spek, A. L.; Elsevier, C. J. *Organometallics* **2010**, *29*, 3109–3116. doi:10.1021/om100435x
24. Huang, D.; Zhao, P.; Astruc, D. *Coord. Chem. Rev.* **2014**, *272*, 145–165. doi:10.1016/j.ccr.2014.04.006
25. Zamora, M. T.; Ferguson, M. J.; McDonald, R.; Cowie, M. *Organometallics* **2012**, *31*, 5463–5477.
26. Vuong, K. Q.; Timerbulatova, M. G.; Peterson, M. B.; Bhadbhade, M.; Messerle, B. A. *Dalton Trans.* **2013**, *42*, 14298–14308. doi:10.1039/C3DT51440D
27. Gu, S.; Xu, H.; Zhang, N.; Chen, W. *Chem. – Asian J.* **2010**, *5*, 1677–1686. doi:10.1002/asia.201000071
28. Lu, C.; Gu, S.; Liu, X. *Inorg. Chem. Commun.* **2014**, *47*, 45–47. doi:10.1016/j.inoche.2014.07.004
29. Gu, S.; Xu, W.; Huang, J. *Prog. Chem.* **2013**, *25*, 330–339. doi:10.7536/PC120746
30. Gu, S.; Huang, J.; Chen, W. *Chin. J. Org. Chem.* **2013**, *33*, 715–737. doi:10.6023/cjoc201301075
31. Gu, S.; Huang, J.; Liu, X.; Liu, H.; Zhou, Y.; Xu, W. *Inorg. Chem. Commun.* **2012**, *21*, 168–172. doi:10.1016/j.inoche.2012.05.007
32. Liu, B.; Zhang, Y.; Xu, D.; Chen, W. *Chem. Commun.* **2011**, *47*, 2883–2885. doi:10.1039/c0cc05260d
33. Chen, C.; Qiu, H.; Chen, W. *J. Organomet. Chem.* **2012**, *696*, 4166–4172. doi:10.1016/j.jorganchem.2011.09.008
34. Lin, J. C. Y.; Huang, R. T. W.; Lee, C. S.; Bhattacharyya, A.; Hwang, W. S.; Lin, I. J. B. *Chem. Rev.* **2009**, *109*, 3561–3598. doi:10.1021/cr8005153
35. Charra, V.; de Frémont, P.; Breuil, P.-A. R.; Olivier-Bourbigou, H.; Braunstein, P. *J. Organomet. Chem.* **2015**, *795*, 25–33. doi:10.1016/j.jorganchem.2015.01.025
36. Liu, B.; Pan, S.; Liu, B.; Chen, W. *Inorg. Chem.* **2014**, *53*, 10485–10497. doi:10.1021/ic501544d
37. Collins, L. R.; Lowe, J. P.; Mahon, M. F.; Poulten, R. C.; Whittlesey, M. K. *Inorg. Chem.* **2014**, *53*, 2699–2707. doi:10.1021/ic4031014
38. Liu, B.; Ma, X.; Wu, F.; Chen, W. *Dalton Trans.* **2015**, *44*, 1836–1844. doi:10.1039/C4DT02986K
39. Liu, B.; Chen, C.; Zhang, Y.; Liu, X.; Chen, W. *Organometallics* **2013**, *32*, 5451–5460. doi:10.1021/om400738c
40. Pouy, M. J.; Delp, S. A.; Uddin, J.; Ramdeen, V. M.; Cochrane, N. A.; Fortman, G. C.; Gunnoe, T. B.; Cundari, T. R.; Sabat, M.; Myers, W. H. *ACS Catal.* **2012**, *2*, 2182–2193. doi:10.1021/cs300544w
41. Catalano, V. J.; Munro, L. B.; Strasser, C. E.; Samin, A. F. *Inorg. Chem.* **2011**, *50*, 8465–8476. doi:10.1021/ic201053t
42. Appukkuttan, P.; Dehaen, W.; Fokin, V. V.; Van der Eycken, E. *Org. Lett.* **2004**, *6*, 4223–4225. doi:10.1021/ol048341v
43. Urankar, D.; Pevec, A.; Turel, I.; Košmrlj, J. *Cryst. Growth Des.* **2010**, *10*, 4920–4927. doi:10.1021/cg100993k
44. Campbell-Verduyn, L. S.; Mirfeizi, L.; Dierckx, R. A.; Elsinga, P. H.; Feringa, B. L. *Chem. Commun.* **2009**, 2139–2141. doi:10.1039/B822994E
45. Chassaing, S.; Sani Souana Sido, A.; Alix, A.; Kumarraja, M.; Pale, P.; Sommer, J. *Chem. – Eur. J.* **2008**, *14*, 6713–6721. doi:10.1002/chem.200800479
46. SMART-CCD Software, Version 4.05; Siemens Analytical X-ray Instruments: Madison, WI, U.S.A., 1996.
47. SHELXS-97 and SHELXL-97, Program for X-ray Crystal Structure Refinement; G. M. Sheldrick: University of Göttingen, Germany, 1997.
48. Spek, A. L. *PLATON, A Multipurpose Crystallographic Tool*; University of Utrecht: Netherlands, 1998.

License and Terms

This is an Open Access article under the terms of the Creative Commons Attribution License (<http://creativecommons.org/licenses/by/2.0>), which permits unrestricted use, distribution, and reproduction in any medium, provided the original work is properly cited.

The license is subject to the *Beilstein Journal of Organic Chemistry* terms and conditions: (<http://www.beilstein-journals.org/bjoc>)

The definitive version of this article is the electronic one which can be found at:
[doi:10.3762/bjoc.12.85](https://doi.org/10.3762/bjoc.12.85)